

ATLAS CP Violation and rare B decays.

V.Nikolaenko¹

¹ *Institute for High Energy Physics, 142281, Protvino, Moscow region, Russian Federation*

On behalf of the ATLAS Collaboration

URL: Vladimir.Nikolaenko@cern.ch

Abstract. A new measurement of CP-violating parameters in $B_s \rightarrow J/\psi\phi$ decay is performed in ATLAS on full Run 1 statistics: $\phi_s = -0.094 \pm 0.083(stat) \pm 0.033(syst.)$ rad. and $\Delta\Gamma_s = 0.082 \pm 0.007$ ps⁻¹. Rare $B_s \rightarrow \mu^+\mu^-$ decay is analyzed on 2011 data at 7 TeV. The ratio of b -quark fragmentation functions measured, $f_s/f_d = 0.240 \pm 0.004(stat.) \pm 0.013(syst.) \pm 0.017(BR)$, this measurement helps to separate contributions from B^0 and B_s mesons into $\mu^+\mu^-$ final state in ongoing analysis on full Run 1 data.

Introduction.

B-physics results are based on statistics acquired mainly with di-muon triggers, with muons of different sign and requirements on muons transverse momentum p_T (mostly 4 GeV/c for both muons, for small fraction of events with high instantaneous luminosity the threshold was increased to 6 GeV/c).

Like the K^0 meson, the B_s meson can be produced in CP-even or CP-odd state with different lifetimes. $\Delta\Gamma_s$ is a difference between inverse lifetimes. CP-odd state has a longer lifetime than the CP-even one, the relative difference is $\sim 13 - 17\%$. There are observed ($b\bar{s} \leftrightarrow \bar{b}s$) oscillations via box diagrams with intermediate u, c, t $q\bar{q}$ -pairs in t -channel and possibly New Physics. The mass difference between heavy (B^H) and light (B^L) CP-eigenstates leads to measured oscillation frequency $\Delta m_s \sim 17.77$ ps⁻¹.

CP-violating phase ϕ_s manifests itself in interference terms between mixing and decay amplitudes. In SM, phase $\phi_s \approx -2\beta_s$, where β_s is an angle in Kobayashi-Maskawa triangle,

$$\beta_s = \arg \frac{-V_{ts}V_{tb}^*}{V_{cs}V_{cb}^*}.$$

SM predictions: $\Delta\Gamma_s = 0.087 \pm 0.021$ ps⁻¹, $\phi_s = -0.0363 + 0.0016 - 0.0015$ rad [1]. Measurements of ϕ_s and $\Delta\Gamma_s$ test theoretical predictions. The analysis of data at 8 TeV is similar for published analysis of 7 TeV data [2]. The number of signal events at 8 TeV is greater by a factor of 3. Due to high statistics, more detailed study of acceptance, signal shape and background was performed. Also Electron tagging was applied. Finally, results at 8 and 7 TeV were statistically combined.

Effects from physics beyond Standard Model can cause a deviation from predicted $BR(B_s \rightarrow \mu^+\mu^-)$. This decay channel was recently observed in LHCb and CMS experiments. LHCb experiment also published interesting observations in differential distributions in $B^0 \rightarrow J/\psi K^*(890)$ decays. Both decays are under investigation in ATLAS, at full Run 1 statistics.

Analysis of $B_s \rightarrow J/\psi\phi$ decay.

The $B_s \rightarrow J/\psi\phi$ is registered in subsequent decays $J/\psi \rightarrow \mu^+\mu^-$ and $\phi \rightarrow K^+K^-$ (without kaon identification). B_s candidates were selected from events with $\mu^+\mu^-$ pair and mass $m(\mu^+\mu^-)$ close to the J/ψ mass. A Vertex fit of $\mu^+\mu^-$ tracks was performed and combined with two other opposite sign charged tracks with transverse momenta $p_T > 1$ GeV and in pseudorapidity interval $|\eta| < 2.5$ taken with kaon mass. Kaon pair candidates with effective mass

¹Caution: the angle β_s is NOT the same as angle β which is associated with another Kobayashi-Maskawa triangle, with d quark instead of s quark.

close to the $\phi(1020)$ mass, in interval $1008.5 < m(\mu^+\mu^-) < 1030.5 \text{ MeV}$ were selected. Then a four-track vertex fit was performed with fixed mass of $\mu^+\mu^-$ pair, and combinations with $\chi^2/NDF < 3.0$ were retained for further analysis. Details of selection requirements can be found in Ref.[2]. With reconstructed B_s vertex and the momentum vector, the primary vertex for lifetime measurement was selected as the vertex with smallest 3-dimensional impact parameter for reconstructed neutral track. Then the proper decay time was calculated:

$\tau = \frac{L_{xy}M_B}{p_{T,H}}$, where L_{xy} denotes the impact parameter in transverse plane to the beam direction and M_B is the World Average mass value. Total 370000 B_s candidates were selected in the mass range from 5.150 to 5.650 GeV and subjected to further analysis.

No decay time cut was applied in the analysis.

Spin-zero B_s meson decays to two vector particles with 3 values of orbital momentum $L = 0, 1, 2$. P-wave decay corresponds to B_s in CP-odd state, while the CP-even state leads to S- and D-waves. Apart from 3 waves mentioned above, a 4-th wave was included in the analysis, where it takes into account the background below the $\phi(1020)$ resonance, with (K^+K^-) system in the S-wave. The last wave corresponds to CP-odd state of B_s meson at the decay time.

A time-dependent Partial Wave Analysis with 4 waves was performed, using 3 angles between final state particles in Transversity basis. The coordinate system is defined as follows. x-axis is an unit vector in the direction of ϕ momentum in J/ψ rest frame, then XY-plane is defined by $\phi \rightarrow K^+K^-$ decay plane with positive projection of K^+ momentum on y-axis, then z-axis is perpendicular to both x and y and z-direction chosen according to convention of positive triplet.

Two polar angles were defined : 1) the ϕ_T is angle between projection of μ^+ momentum vector on (x,y) plane in the J/ψ rest frame and x-axis; 2) the ψ_T is angle between x-axis and K^+ momentum in the ϕ rest frame. The 3-rd θ_i angle is the angle between z-axis and μ^+ momentum vector in $J/\psi\phi$ rest frame.

A multi-dimensional fit to the data determine the following physical parameters: four amplitudes ($A_0, A_{perp}, A_{par}, A_S$), strong phases ($\delta_0, \delta_{perp}, \delta_{par}, \delta_S$, one of them can be fixed), as well as the mass of the B_s meson $m(B_s)$, ϕ_S , $\Delta\Gamma_S$ and the average inverse lifetime Γ_S . The mass spectrum used for separation of B_s signal from background, which is mainly the combinatorial one. There is also a small BG component from $B^0 \rightarrow J/\psi K^*$ decay due to the absence of pion identification.

An important ingredient of the analysis is tagging of b or \bar{b} quark in B_s meson at the production time. The b -quark charge tagging significantly improves the precision of the ϕ_s measurement and helps in measurement of strong phases and resolution of ambiguous solutions. If the tagging information is available, then new oscillating terms appear in time-dependent functions in partial waves, and amplitudes of new terms are proportional to $\sin(\phi_s)$. It is known that the absolute value of ϕ_s angle is small, and new terms significantly improve the measurement precision. Information from opposite side tagging is used, i.e. leptons and/or jet charge from decay of 2nd B-hadron in the event. Methods were calibrated on B^{+-} -candidates in data after BG subtraction. Apart from methods based on combined muons, tagged muons and the jet charge used in the analysis of 7 TeV data, a new tagging method on electrons was developed and used in the analysis of data acquired at 8 TeV . Opposite-side charge distributions for different methods shown in Fig. 1, separately for B^+ and B^- calibration samples. Table 1 specifies the tagging power of different methods.

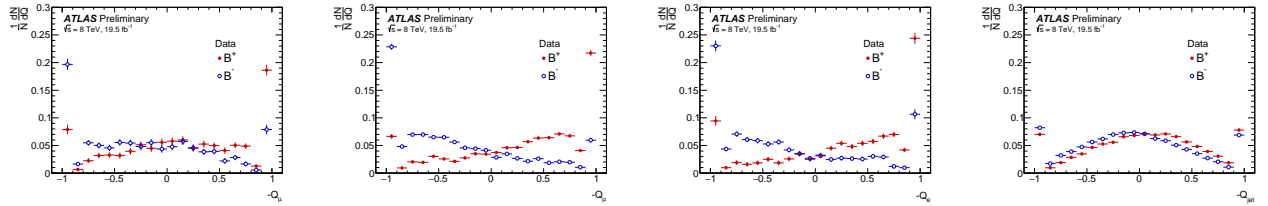


FIGURE 1. The opposite-side muon cone charge distribution for B^{+-} signal candidates for segment-tagged (left); combined muon (next); electron cone (next); jet charge(right)

Efficiency of B_s candidate reconstruction was estimated in specially tuned Monte Carlo (MC) procedure, in several bins on transverse momentum p_T and pseudorapidity η .

A fit model was constructed and physical parameters were determined at the result of unbinned likelihood fit. A signal component of fit model contains a mass term (a Tripple Gaussian function), angular functions and time-dependent functions. Angular functions (4 diagonal and 6 non-diagonal) are multiplied by time-dependent functions

TABLE 1. Tagging power of different methods.

Tagger	Tagging Power [%]
Combined muon	0.92 ± 0.02
Electron	0.29 ± 0.01
Tagged muon	0.10 ± 0.01
Jet charge	0.19 ± 0.01
Total	1.49 ± 0.02

with dependencies on two exponential functions (smeared with experimental resolution) and also terms with tagging probability distributions. Detailed description of angular and time-dependent function can be found in Ref. [1].

A background component of the Fit model consists of two parts, a combinatorial background component and a B^0 component. Combinatorial component contains a mass term (an exponential function). A time-dependent component contains 2 prompt exponents (including a tail to negative lifetime due to experimental resolution) and two non-prompt exponential functions. It worth mentioning that the error on time measurements was taken from reconstruction results in individual events and then multiplied by a scaling factor, which was also included as a fit parameter. This parameter was determined from the negative tail in time distributions of the data, due to absence of the lifetime cut. The angular distributions in this component were determined from fits in mass side bands. Finally, the differences in tagging efficiency and lifetime uncertainties between signal and background regions were taken into account in so called Punzi terms.

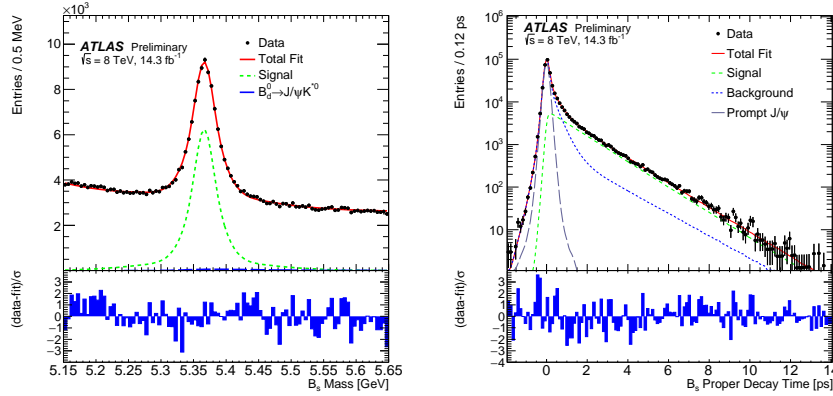


FIGURE 2. (Left) Mass fit projection for the $B_s^0 \rightarrow J/\psi\phi$. The red line shows the total fit, the dashed green line shows the signal component while the dotted blue line shows the contribution from $B^0 \rightarrow J/\psi K^*$ events. (Right) Proper decay time fit projection for the $B_s^0 \rightarrow J/\psi\phi$. The red line shows the total fit while the green dashed line shows the total signal. The total background is shown as a blue dashed line with a grey dotted line showing the prompt J/ψ background. Below each figure is a ratio plot that shows the difference between each data point and the total fit line divided by the statistical uncertainty (σ) of that point.

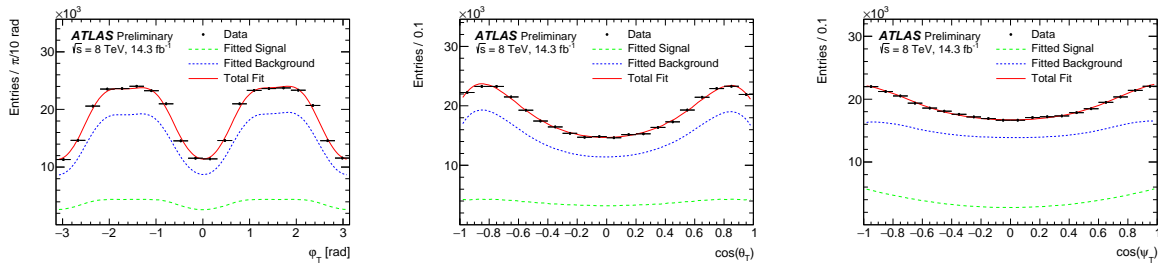


FIGURE 3. Fit projections for transversality angles. (Left): ϕ_T , (Right): $\cos(\theta_T)$, (Center): $\cos(\psi_T)$. In all three plots, the red line shows the total fit, the dashed green line shows the signal component and the dotted blue line shows the background contribution.

TABLE 2. Summary of systematic uncertainties assigned to the physics parameters.

	ϕ_s [rad]	$\Delta\Gamma_s$ [ps ⁻¹]	Γ_s [ps ⁻¹]	$ A_{\parallel}(0) ^2$	$ A_0(0) ^2$	$ A_S(0) ^2$	δ_{\perp} [rad]	δ_{\parallel} [rad]	$\delta_{\perp} - \delta_S$ [rad]
Tagging	0.026	0.003	$<10^{-3}$	$<10^{-3}$	$<10^{-3}$	0.001	0.238	0.014	0.004
Acceptance	$<10^{-3}$	$<10^{-3}$	$<10^{-3}$	0.003	$<10^{-3}$	0.001	0.004	0.008	$<10^{-3}$
Background angles model:									
Choice of p_T bins	0.02	0.006	0.003	0.003	$<10^{-3}$	0.008	0.004	0.006	0.008
Choice of mass interval	0.008	0.001	0.001	$<10^{-3}$	$<10^{-3}$	0.002	0.021	0.005	0.003
B_d^0 background model	0.008	$<10^{-3}$	$<10^{-3}$	0.001	$<10^{-3}$	0.008	0.007	$<10^{-3}$	0.005
Fit model:									
Default fit	0.001	0.002	$<10^{-3}$	0.002	$<10^{-3}$	0.002	0.025	0.015	0.002
Mass Signal model	0.004	$<10^{-3}$	$<10^{-3}$	0.002	$<10^{-3}$	0.001	0.015	0.017	$<10^{-3}$
Mass Background model	$<10^{-3}$	0.002	$<10^{-3}$	0.002	$<10^{-3}$	0.002	0.027	0.038	$<10^{-3}$
Time Resolution model	0.003	$<10^{-3}$	0.001	0.002	$<10^{-3}$	0.002	0.057	0.011	0.001
Total	0.036	0.007	0.003	0.006	0.001	0.013	0.25	0.05	0.01

Concerning the B^0 background component, the mass term was described by a Landau function with parameters tuned in a MC procedure. An exponential function smeared with per-candidate errors describes the time dependence, with lifetime value taken from PDG [3]. Angular distributions: taken from 3-dimensional fits to MC.

The mass fit projection and proper lifetime fit projection are shown at Fig.2. Fig.3 demonstrates fit projections for transversity angles. Table 2 presents a list of considered sources of systematics and preliminary evaluation of systematic errors for physics parameters.

It worth mentioning that the correlations between physics parameters are small, the largest correlation term between $\Delta\Gamma_s$ and Γ_s parameters is close to 0.4. Correlation between $(\phi_s, \Delta\Gamma_s) = 0.110$.

The following results were obtained from the analysis of data at 8 TeV :

$\phi_s = -0.119 \pm 0.088(stat.) \pm 0.036(syst.) rad.. \Delta\Gamma_s = 0.096 \pm 0.013(stat.) \pm 0.007(syst.) ps^{-1}$.

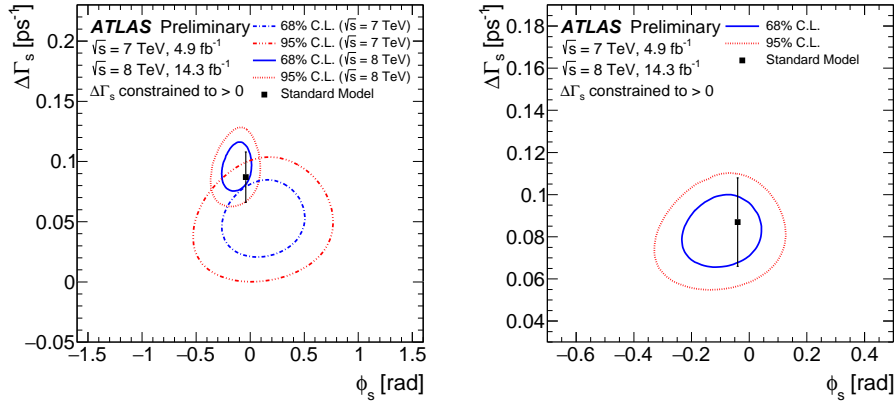


FIGURE 4. Likelihood contours in the $\phi_s - \Delta\Gamma_s$ plane for individual results from 7 TeV and 8 TeV data (left) and a final statistical combination of the results from 7 TeV and 8 TeV data (right). The blue line shows the 68% likelihood contour, while the red dotted line shows the 95% likelihood contour (statistical errors only). Points with errors indicate predictions from parametrisation in Standard Model.

At the next step, the results obtained on the data at 7 and 8 TeV were statistically combined. A Best Linear Unbiased Estimate (BLUE) procedure was used. A conservative approach was applied in treatment of correlations between systematic errors, assuming no correlations or 100% correlations and adding a difference to the final systematic error. Comparison between measurements at 7 and 8 TeV for ϕ_s and $\Delta\Gamma_s$ is presented in Fig.4, as well as the combined result. One can see that the analysis at 8 TeV yields more precise results in comparison with previous analysis at 7 TeV.

TABLE 3. Combined results for physics parameters.

Parameter	Value	Stat. err.	Syst. err.	
ϕ_s	-0.094	0.083	0.033	rad.
$\Delta\Gamma_s$	0.082	0.011	0.007	ps ⁻¹
Γ_s	0.677	0.003	0.003	ps ⁻¹
$ A_{\text{para}}(0) ^2$	0.227	0.004	0.006	
$ A_0(0) ^2$	0.515	0.004	0.002	
$ A_S(0) ^2$	0.086	0.007	0.012	
δ_{perp}	4.13	0.34	0.15	rad.
δ_{para}	3.16	0.13	0.05	rad.
$\delta_{\text{perp}} - \delta_s$	-0.08	0.03	0.01	rad.

Combined results for physics parameters are presented in Table 3.

Comparison of ATLAS Run 1 result with combination of other measurements is shown at Fig.5(left). Recent results from LHCb and CMS experiments can be found in Refs. [4, 5].

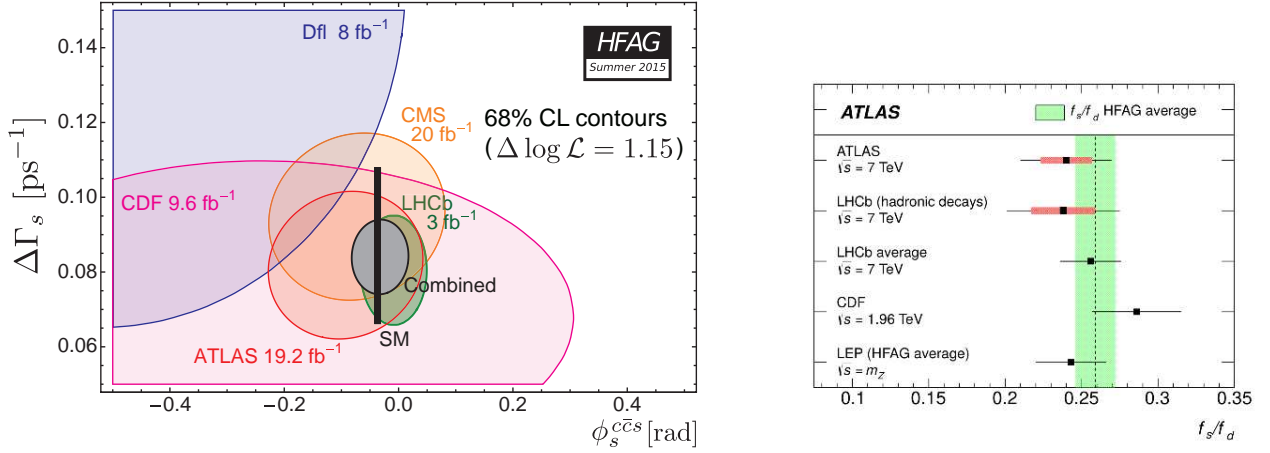


FIGURE 5. (Left) 68% conf. level contours in $(\phi_s, \Delta\Gamma_s)$ plane of ATLAS, CMS, CDF, D0 and LHCb results and their combined contour, as well as the Standard Model predictions (thin black rectangle). Taken from [6]. (Right) Compilation of measurements of b -quark fragmentation functions f_s/f_d .

Status of Rare decay studies in ATLAS.

Decays $B_s \rightarrow \mu^+\mu^-$ and $B^0 \rightarrow \mu^+\mu^-$ are suppressed in SM.

Recent predictions in SM: $BR(B_s \rightarrow \mu^+\mu^-) = (3.65 \pm 0.23) \times 10^{-9}$, $BR(B^0 \rightarrow \mu^+\mu^-) = (1.06 \pm 0.09) \times 10^{-10}$ [7].

Combined result from LHCb and CMS is recently published [8]:

$$BR(B_s \rightarrow \mu^+\mu^-) = (2.8_{-0.6}^{+0.7}) \times 10^{-9}, \quad BR(B^0 \rightarrow \mu^+\mu^-) = (3.9_{-1.4}^{+1.6}) \times 10^{-10}.$$

ATLAS experiment put a limit on 7 TeV data with integrated luminosity of 4.9 fb⁻¹ [9, 10]

$$BR(B_s \rightarrow \mu^+\mu^-) < 19 \times 10^{-9} \text{ at 90\% conf. level.}$$

ATLAS analysis on full Run 1 statistics ongoing, more precise result expected soon.

A particular challenge in these analyses is a problem of separation of signals from B_s and B^0 decays, which have close masses and are not well resolved. A supplementary study in this direction is completed in ATLAS, the Determination of ratio of b -quark fragmentation functions f_s/f_d . Exclusive decays $B_s \rightarrow J/\psi\phi$ and $B^0 \rightarrow J/\psi K^{*0}(890)$ were used from data with integrated luminosity of 2.47 fb⁻¹ at $\sqrt{s} = 7$ TeV. A theoretical calculation of Branching Fractions ratio $BR(B_s \rightarrow J/\psi\phi)/BR(B^0 \rightarrow J/\psi K^{*0}(890))$ from Ref. [11] was used. With $6640 \pm 100 \pm 220$ reconstructed $B_s \rightarrow J/\psi\phi$ and $36290 \pm 320 \pm 650$ $B^0 \rightarrow J/\psi K^{*0}$ decays, the following ratio of fragmentation functions in kinematical region $p_T > 8$ GeV was obtained:

$$f_s/f_d = 0.240 \pm 0.004(stat.) \pm 0.013(syst.) \pm 0.017(branching).$$

Comparison of this result with other measurements presented at Fig.5(right).

Study of other semi-rare decay, $B^0 \rightarrow \mu^+\mu^-K^{*0}$ in ATLAS with full Run 1 statistics is ongoing.

Summary

ATLAS can provide precise measurements in B-decays, which are relevant for searches of effects beyond SM:

- CP-violating phase ϕ_s and decay width difference $\Delta\Gamma_s$ measured in 2012 data at 8 TeV;
- statistical combination performed for 2011+2012 data ($4.6 + 14.3fb^{-1}$),
 $\phi_s = -0.094 \pm 0.083(stat.) \pm 0.033(syst.) rad$;
 $\Delta\Gamma_s = 0.082 \pm 0.011 \pm 0.007 ps^{-1}$;
- obtained results are consistent with SM predictions and other experiments.
- $B_s \rightarrow \mu^+\mu^-$ decay analyzed 2011 data, full Run 1 result expected soon;
- The ratio of b-quark fragmentation functions measured at $p_T > 8 GeV/c$, $f_s/f_d = 0.240 \pm 0.004(stat.) \pm 0.013(syst.) \pm 0.017(branching)$;
- analysis of $B_d \rightarrow J/\psi K^{*0}$ decay on full Run 1 is ongoing;

Statistical errors dominate in measurements, we expect better precision from the future Run 2 data due to modifications in the ATLAS detector (most notably the IBL) and significantly more statistics.

ACKNOWLEDGMENTS

This work was supported in part by the Russian MES grant RFMEFI61014X0005 and Presidential Grant NSh-999.2014.2.

REFERENCES

- [1] J.Charles et al., Predictions of selected flavor observables within the standard model Phys. Rev. D 84 (2011), 033005
- [2] ATLAS collaboration, Flavor tagged time-dependent angular analysis of the $B_s \rightarrow J/\psi$ decay and extraction of $\Delta\Gamma_s$ and the weak phase ϕ_s in ATLAS, Phys. Rev. D90 (2015) 5, 052007, arXiv:1407.1796
- [3] The Review of Particle Physics, K.A. Olive et al. (Particle Data Group), PDG Chinese Phys C V38 Number 9 September 2014
- [4] LHCb collaboration, R Aaij et al., Precision measurement of CP violation in $B_s \rightarrow J/\psi K^+ K^-$ decays, Phys.Rev. Lett. 114 (2015) 041801, arXiv:1411.3104
- [5] CMS collaboration, Measurement of the CP-violating weak phase ϕ_s and the decay width difference $\Delta\Gamma_s$ using the $B_s \rightarrow J/\psi\phi(1020)$ decay channel, Tech.Rep. CMS-PAS-BPH-13-012, CERN, Geneva, 2014, arXiv:1507.07527, submitted to PL B
- [6] Y. Amhis et al. (Heavy Flavour Averaging Group), Averages of b -hadron, c -hadron, and τ -lepton properties of summer 2014, arXiv:1412.7515 [hep-ex] and online update at <http://www.slac.stanford.edu/xorg/hfag> [www.slac.stanford.edu]
- [7] C.Bobeth et al., $B_{s,d} \rightarrow l^+l^-$ in the Standard Model with Reduced Theoretical Uncertainty, PRL 112,101801 (2014)
- [8] CMS collaboration, LHCb collaboration, Observation of the rare $B_s^0 \rightarrow \mu^+\mu^-$ decay from combined analysis of CMS and LHCb data, Nature 522 (2015) 68, and ref. therein
- [9] ATLAS collaboration, Limit on $B_s^0 \rightarrow \mu^+\mu^-$ branching fraction based on $4.9 fb^{-1}$ of integrated luminosity, ATLAS-CONF-2013-076, <http://cds.cern.ch/record/1562934>
- [10] ATLAS collaboration, Search for the decay $B_s^0 \rightarrow \mu^+\mu^-$, Phys. Lett. B713 (2012) 387, arXiv:1204.0735
- [11] Xin Lio et al., Penguin pollution $B \rightarrow J/\psi V$ decays and impact on the $B_s - \bar{B}_s$ mixing phase, Phys. Rev. 89, 094010 (2014).